Electronic Supplementary Information (ESI)

Synergetic contribution of fluorinated azide for high EQE and operational stability of top-illuminated, semitransparent, photomultiplication-type organic photodiodes

Juhee Kim,‡[a] Chul Woong Joo,‡[b,c] Syed Zahid Hassan,[a] Seong Hoon Yu,[a] Mingyun Kang,[a] Jae-Eun Pi,[b] Seung-Youl Kang,[b] Young-Sam Park*[b] and Dae Sung Chung*[a]

[a] Department of Chemical Engineering, Pohang University of Science and Technology (POSTECH), Pohang 37673, Republic of Korea

[b] Flexible Device Research Group, Electronics and Telecommunications Research Institute (ETRI), 218 Gajeong-ro, Yuseong-gu, Daejeon 34129, Republic of Korea

[c] School of Chemical Engineering, Sungkyunkwan University, 2066, Seobu-ro, Jangan-gu, Suwon, Gyeonggi 16419, Republic of Korea

* Correspondence: s_yspark@etri.re.kr (Y.-S. Park)

* Correspondence: dchung@postech.ac.kr (D. S. Chung)

Experimental Section

Materials

P3HT and $PC_{71}BM$ were purchased from RIEKE METALS and 1-Material, respectively. PEIE, Mucasol, acetone, isopropanol, and DCB were purchased from Sigma-Aldrich. MoO_3 was purchased from Alfa Aesar. All chemicals were used as received without further purification processes. bisFPA was synthesized following the previous report.[1]

Device Fabrication

To fabricate PM-OPDs, ITO-patterned glass substrates were cleaned by sequential sonication in a Mucasol solution, distilled water, acetone, and isopropanol, followed by O_2-plasma treatment for 10 min. To prepare interlayer of the devices, PEIE was diluted in 2-methoxyethanol with a concentration of 0.35–0.40 wt%. The prepared PEIE solution were spin-coated on top of the O_2-plasma-treated ITO substrates at 5,000 rpm, followed by thermal treatment at 130 °C for 20 min to evaporate the residual solvent. The P3HT:$PC_{71}BM$:bisFPA blend solutions were prepared with various ratios of bisFPA (100:1:0, 100:1:5, 100:1:10, in wt%) by dissolving in DCB at a concentration of 40 mg mL^{-1}. The solutions were stirred at 80 ºC for 24 h, then spin-coated at 1,000 rpm on top of PEIE layers, and thermally annealed at 150 °C for 20 min in a nitrogen-filled glove box. For the bisFPA-embedded device, the deposited active layers were exposed to UV (254 nm) light for 10 min prior to the annealing step. MoO_3/Au/MoO_3 electrodes were deposited onto the active layers by thermal evaporation under high vacuum. The photoactive area of the fabricated devices is 0.09 cm^2.

Device Characterization

UV-Vis absorption spectra were measured using Cary 5000 spectrophotometer. The sheet resistance of the top electrodes was measured using a 4-point probe at ambient temperature. *J*–*V* characteristics and EQE spectra were measured by a combination of Keithley 2450 SourceMeter and an Oriel Cornerstone 130 1/8 m monochromator controlled by LabView program. For noise current measurements, a Stanford Research SR570 current pre-amplifier and Agilent 35670A spectrum analyzer was used. An atomic depth profiles were measured using SIMS (IMS 6F, CAMECA). The SCLC analyses were performed with the geometry of ITO/PEDOT:PSS/photoactive layer/MoO_3/Au and ITO/PEIE/photoactive layer/LiF/Al for hole-only and electron-only devices, respectively. The theoretical fitting was provided by the SCLC equation of $J=9\varepsilon\varepsilon_0\mu(V\text{-}V_{bi})^2/8d^3$, where ε is the relative permittivity of the thin film, ε_0 is the permittivity of free space, μ is the charge carrier mobility, and d is the thin film thickness.[2] The LDR was measured by two light sources with various optical filters: monochromatized lights (445 nm or 520 nm for top/bottom illumination, respectively) and lasers (445 nm or 520 nm), and calculated using the equation of $LDR=20\log P_{max}/P_{min}$, where P_{max}, P_{min} are the maximum and minimum values of the detectable power density, respectively. The −3-dB cut-off frequency was measured using a TDS5052 digital phosphor oscilloscope (Tektronix) and an optically filtered laser diode in connection with a Tektronix AFG310 arbitrary function generator. For DH stability test, purified water was incorporated in the airtight container to keep 85% RH, and the devices were placed on a hotplate maintained at 85 ºC in dark conditions. The surface morphology of the film was characterized using AFM (XE-150, Park Systems) and a digital microscope (VHX-900F, Keyence).

300 ppi fingerprint sensor fabrication

Bottom-gate bottom-contact (BGBC) oxide thin film transistor (TFT) array was fabricated in 6-inch fab at Electronics and Telecommunications Research Institute. The TFT structure is: molybdenum (Mo, 100 nm, gate)/indium tin oxide (ITO, 150 nm, source and drain)/indium gallium zinc oxide (IGZO, 30 nm, active layer). Silicon oxide (200 nm, passivation), Mo (100 nm, metal anode), and ITO (50 nm, anode) were subsequently deposited on the IGZO active layer. Finally, the OPD organic layers were formed on the ITO anode, and Al_2O_3 thin film encapsulation was performed.

Synthesis and characterization of bisFPA

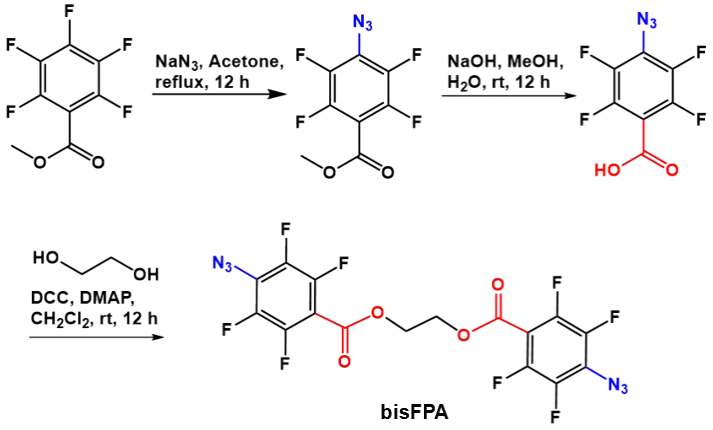

Characterization of synthesized bisFPA

The bisFPA was characterized by NMR spectroscopy. ^{1}H NMR and ^{19}F NMR were measured by Bruker Avance 400 with deuterated chloroform ($CDCl_3$) as solvent.

Materials

Methyl pentafluorobenzoate, sodium azide and 4-(dimethylamino)pyridine (DMAP) were purchased from TCI. Sodium hydroxide (NaOH), hydrochloric acid (HCl), N,N'-dicyclohexylcarbodiimide (DCC) (1.0 M in methylene chloride), $CDCl_3$, acetone, methanol and anhydrous dichloromethane were purchased from Sigma Aldrich. $MgSO_4$, n-hexane, ethyl acetate (EtOAc) and diethylether were purchased from Daejung Chemicals Korea.

Synthesis of methyl 4-azido-2,3,5,6-tetrafluorobenzoate

The methyl pentafluorobenzoate (5 g, 22.11 mmol) was dissolved in a mixture of acetone (60 mL) and water (30 mL) under stirring condition. Then sodium azide was added slowly (2.16 g, 33.17 mmol) to the reaction flask. After refluxing at 60 °C for 12 hours, the reaction mixture was cooled down to room temperature. Then reaction mixture was extracted with diethyl ether and solvents were removed by distillation at a reduced pressure. The completion of reaction was confirmed by checking TLC. Crude product was used for next step without characterization.

Synthesis of 4-azido-2,3,5,6-tetrafluorobenzoic acid

To the solution of 4-azido-2,3,5,6-tetrafluorobenzoate (2 g, 8.03 mmol) in methanol (50 mL) and water (5 mL), aqueous solution of NaOH (20 % w/w, 12.04 mmol, 1.5 equivalents) were added in the reaction flask. Solution was stirred overnight at room temperature followed by neutralization with HCl (2 M) by adjusting pH to ~1. Reaction mixture was extracted with diethyl ether and solvents were removed by distillation at a reduced pressure. The completion of reaction was confirmed by checking TLC which yielded more polar product. Crude product was used for next step without characterization.

Synthesis of ethane-1,2-diyl bis(4-azido-2,3,5,6-tetrafluorobenzoate), bisFPA

A mixture of 4-azido-2,3,5,6-tetrafluorobenzoic acid (1 g, 4.25 mmol) and ethylene glycol (107 μL, 1.91 mmol) were dissolved in anhydrous dichloromethane (25 mL) under stirring at room temperature followed by addition of DMAP (51 mg, 0.42 mmol). After 30 minutes, temperature was lowered to 0 °C, and DCC (1 M in dichloromethane) (4.67 mL, 4.67 mmol) was added under N_2 atmosphere. After 12 h, the reaction mixture was neutralized with water and extracted with dichloromethane and solvents were removed by distillation at a reduced pressure. The resulting crude product was purified by silica gel column chromatography using an eluent of ethyl acetate/n-hexane (1/5), which yielded the bisFPA as a colorless solid (560 mg, 58 %). ^{1}H NMR (400 MHz, $CDCl_3$): δ = 4.71 (s, 4H). ^{19}F NMR (376.5 MHz, $CDCl_3$): δ = -138.16 -138.25 (m), -150.69 -150.80 (m). ^{1}H NMR and ^{19}F NMR of synthesized bisFPA matches with previously reported value.[3]

^{1}H NMR

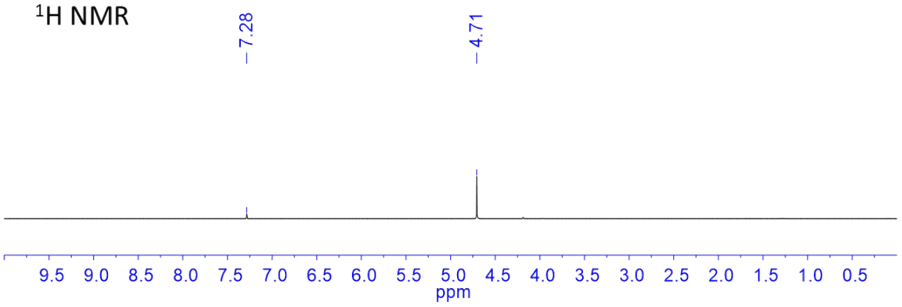

^{19}F NMR

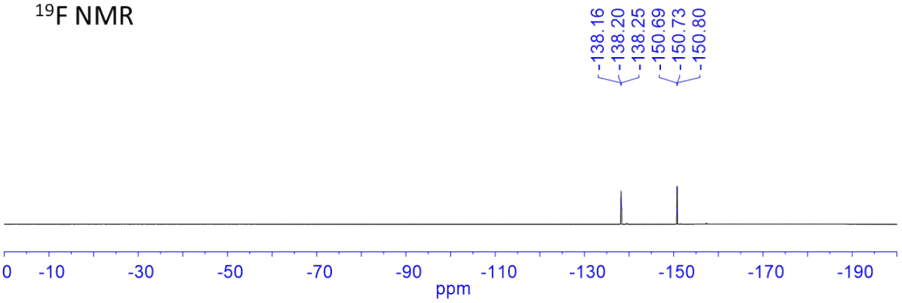

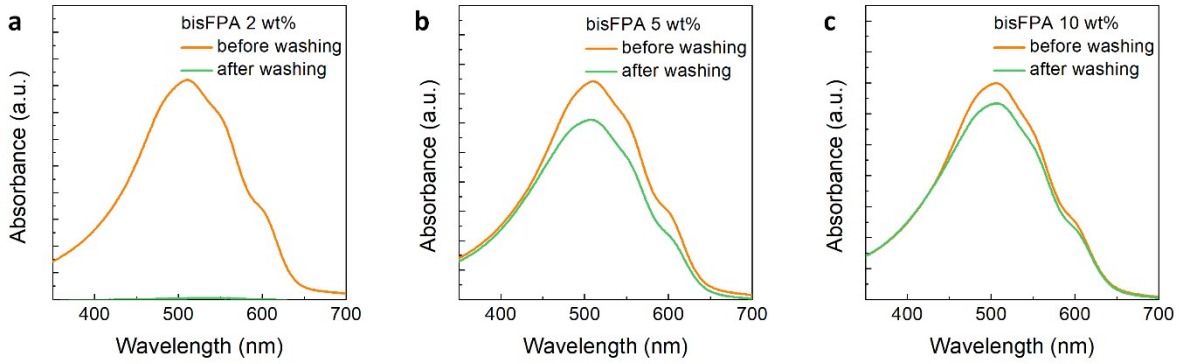

Fig. S1 UV-Vis absorption spectra of P3HT:$PC_{71}BM$ (100:1, in wt%) films with different contents of bisFPA before and after washing with DCB. Note that in the actual device fabrication procedure, washing process was not performed.

Table S1. Summary of 2D-GIXD parameters for P3HT:$PC_{71}BM$ (100:1, in wt%) films with different contents of bisFPA on PEIE layers.

Contents of bisFPA	Lamellar stacking distance (Å)	π–π stacking distance (Å)	$g_{(010)}$ (%)
0 wt%	16.21	3.86	18.41
5 wt%	16.54	3.87	18.28
10 wt%	16.62	3.90	21.66

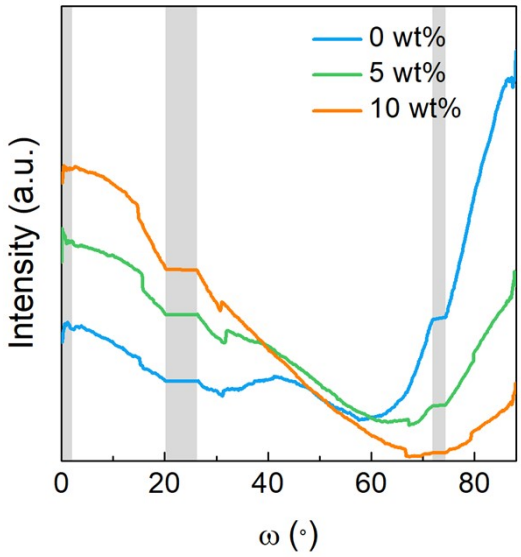

Fig. S2. Pole figure analysis for π–π stacking of P3HT:$PC_{71}BM$ (100:1, in wt%) films with different contents of bisFPA.

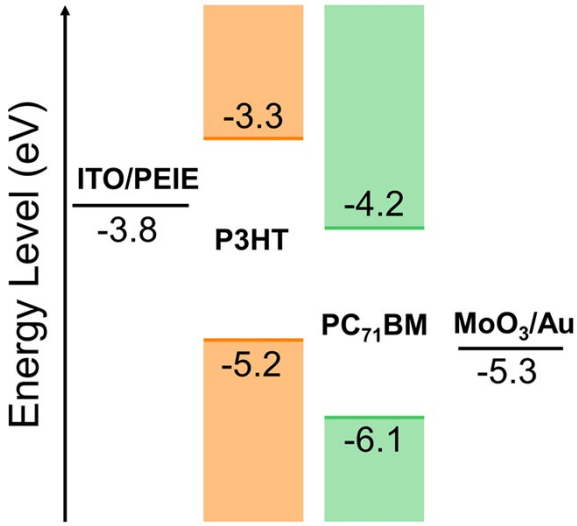

Fig. S3. Energy level diagram of the designed PM-OPD structure.

Top electrode optimization

To optimize the dielectric/metal/dielectric (DMD) structure as a transparent and conductive top electrode, the effect of varying the thickness of the top molybdenum oxide (MoO_3) layer while fixing the thickness of the bottom MoO_3 as 5 nm for efficient charge extraction was studied. The generalized transfer matrix method (GTMM) was employed to optimize the thickness of the top MoO_3. Based on the experimentally obtained reflective index (*n*) and the extinction coefficient (*k*) values of MoO_3 and Au, the simulated transmittance spectra of the MoO_3/Au/MoO_3 structure as a function of the top MoO_3 thickness are shown in Fig. S4a. It can be seen that the transmittance in the NIR range increases with the thickness of the top MoO_3 layer, accompanied by the simultaneous gradual quenching of the visible transmittance. The optimal thickness of the top MoO_3 which preserves balanced transmittance in the visible and NIR ranges was determined as 40 nm. Next, to optimize the electrical conductivity of the MoO_3/Au/MoO_3 DMD electrode, the thickness of the Au layer was varied, and the transmittance spectra as a function of Au thickness are shown in Fig. S4b. In addition, the corresponding sheet resistance and transmittance at 600 nm were summarized in Fig. S4c. The sheet resistance sharply decreased with increasing Au thickness, while the peak transmittance increased slightly and was maximized at Au thickness of 9 nm. The optimal thickness of Au was hence chosen as 9 nm with a sufficiently low sheet resistance value of 10.6 Ω sq^{-1} as well as high peak transmittance of 87.3% at 646 nm.

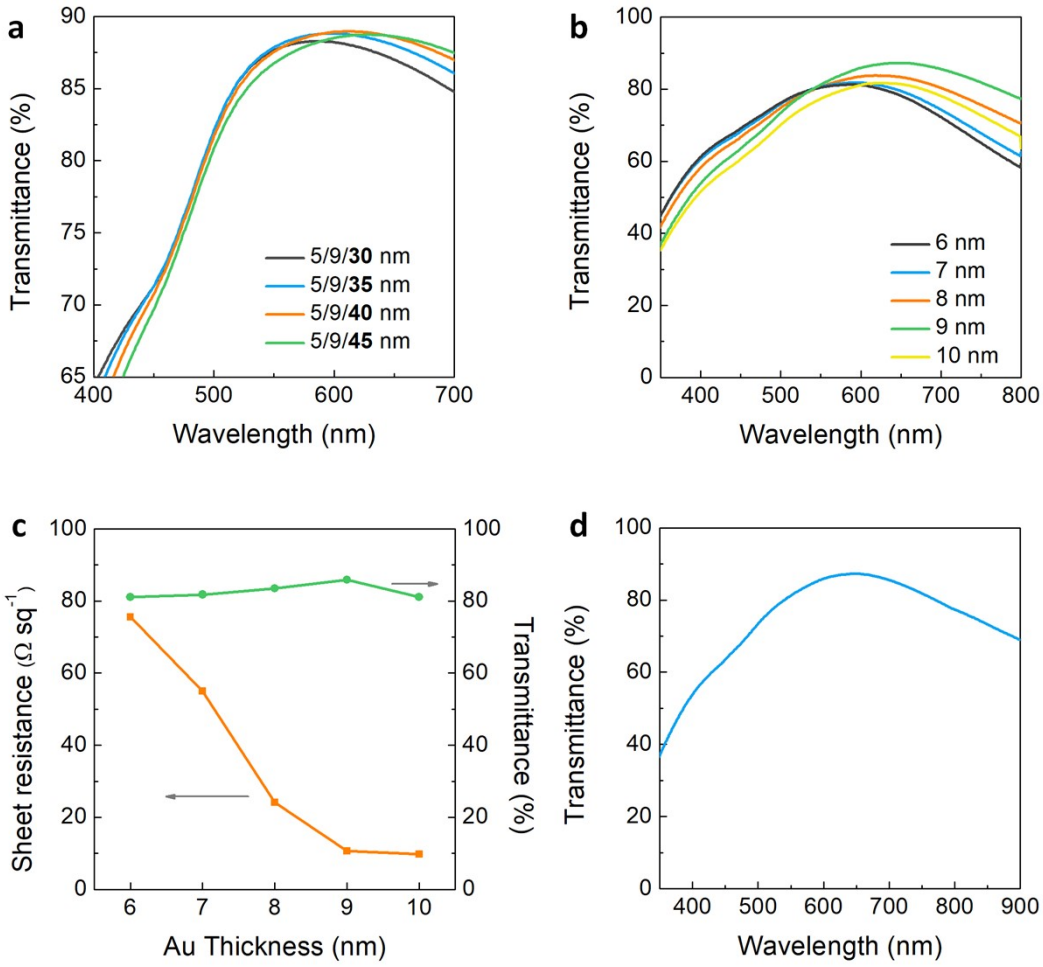

Fig. S4. (a) Simulated transmittance spectra of the DMD structure as a function of the top MoO_3 thickness. (b) Measured transmittance spectra of the MoO_3/Au/MoO_3 (5 nm/*x* nm/40 nm) structure as a function of Au thickness. (c) Sheet resistance and transmittance at 600 nm of the MoO_3/Au/MoO_3 (5 nm/*x* nm/40 nm) structure as a function of the Au thickness. (d) Measured transmittance spectrum of the optimized DMD structure with thickness of MoO_3/Au/MoO_3 (5 nm/9 nm/40 nm).

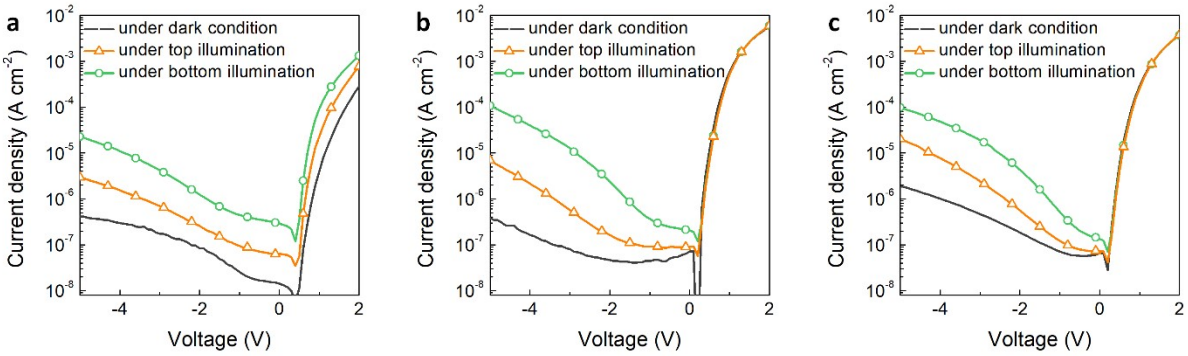

Fig. S5. (a-c) *J–V* characteristics of PM-OPDs without bisFPA (a), with 5 wt% bisFPA (b), and with 10 wt% bisFPA (c) under dark, top (600 nm, 6.61 × 10^{-6} W cm^{-2}) and bottom (520 nm, 8.28 × 10^{-6} W cm^{-2}) illumination conditions.

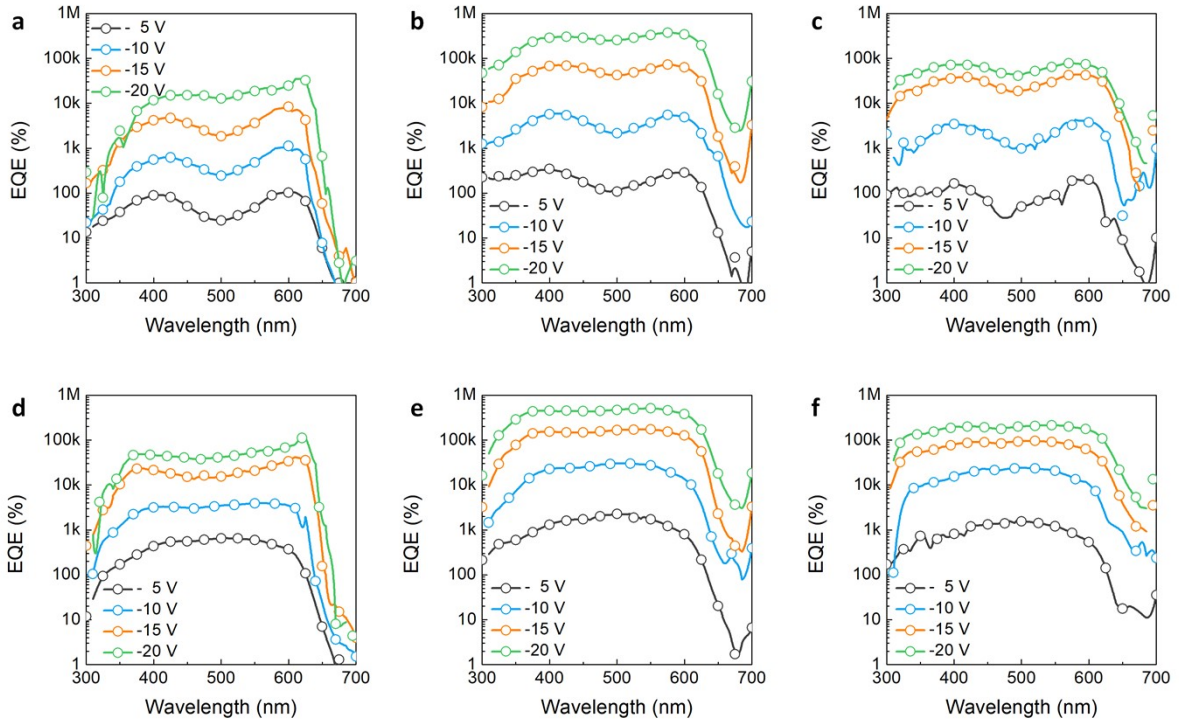

Fig. S6. (a-c) EQE spectra of PM-OPDs without bisFPA (a), with 5 wt% bisFPA (b), and with 10 wt% bisFPA (c) at various reverse biases under top illumination. (d-f) EQE spectra of PM-OPDs without bisFPA (d), with 5 wt% bisFPA (e), and with 10 wt% bisFPA (f) at various reverse biases under bottom illumination.

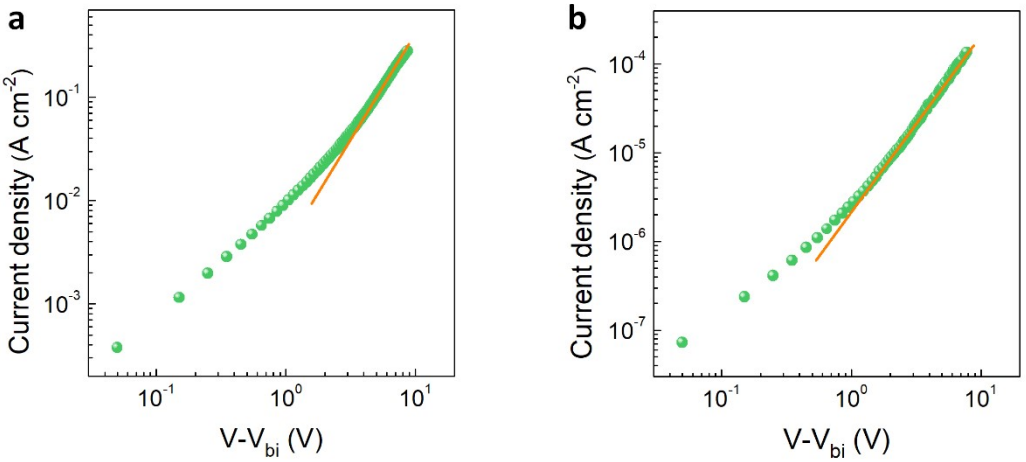

Fig. S7. (a,b) Space-charge-limited current analyses of hole-only (a) and electron-only (b) devices.

Table S2. Summary of parameters used in the drift-diffusion simulations.

Temperature (K)	290
Thermionic work function of the cathode[a] **(eV)**	4.45
Thermionic work function of the anode (eV)	5.00
HOMO level (eV)	5.30
LUMO level (eV)	3.30
N_0[b] **(m^{-3})**	10^{29}
Dielectric constant	3
Charge carrier mobilities ($cm^2 V^{-1} s^{-1}$)	μ_e: 5×10^{-8}, μ_h: 1×10^{-4}
Trap density[b] **(cm^{-3})**	10^{18}
Trap energy depth (eV)	0.565 (without bisFPA) or 0.680 (with bisFPA)
Electron/hole capture rate[b] **($cm^3 s^{-1}$)**	10^{-13}
Langevin recombination efficiency[c]	1
Non-radiative decay rate[c] **(s^{-1})**	10^5
Generation efficiency[c]	1
Diffusion constant[c] **($cm^2 s^{-1}$)**	0
Annihilation rate[c] **($cm^3 s^{-1}$)**	0
Optical generation efficiency[c]	0.66
Pair separation[c] **(nm)**	1.285
Charge transfer type[c]	Onsager–Braun
Wavelength (nm)	550 (single wavelength)
Light intensity ($W cm^{-2}$)	7.95×10^{-6}

[a] Work function value larger than that of under dark condition was used because of the pseudo-Ohmic junction induced by the trapped electrons near the cathode.[4-6]

[b] Parameters used in Reference 7.

[c] Parameters used in References 8,9.

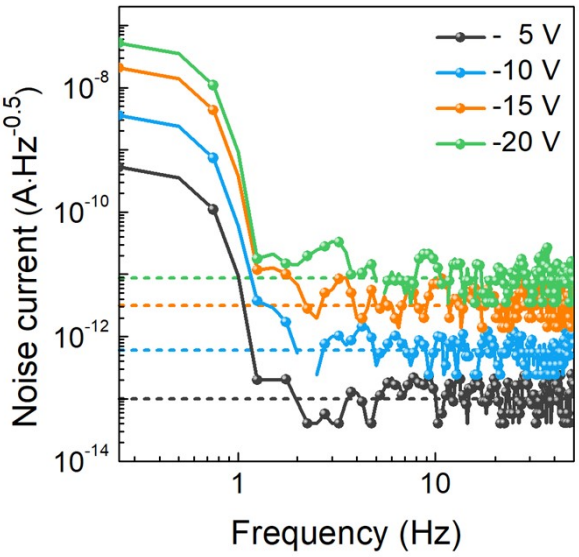

Fig. S8. Noise current spectra of the optimized PM-OPD with bisFPA under various reverse biases.

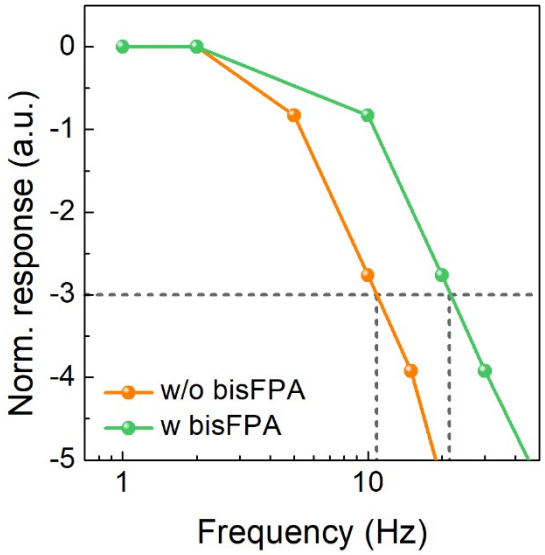

Fig. S9. Bode plots of the PM-OPDs with and without bisFPA under a green (520 nm) light illumination with intensity of 8.28 μW cm^{-2} measured under −20 V.

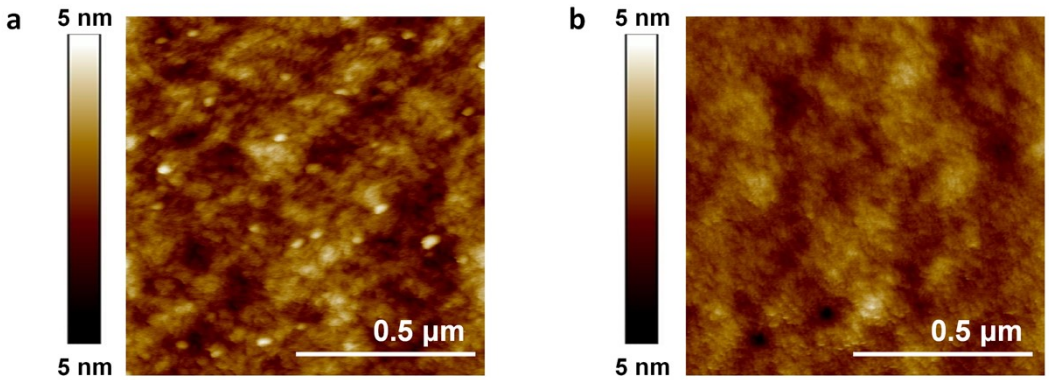

Fig. S10. (a,b) AFM topographical image of P3HT:$PC_{71}BM$:bisFPA (100:1:5, in wt%) film before (a) and after (b) damp heat (85°C/85% RH) test for 120 h.

Reference

1. M. Sundhoro, J. Park. B. Wu, M. Yan, *Macromolecules*, 2018, **51**, 4532.
2. H. T. Nicolai, G. A. H. Wetzelaer, M. Kuik, A. J. Kronemeijer, B. de Boer, P. W. M. Blom, *Appl. Phys. Lett.*, 2010, **96**, 172107.
3. M. J. Kim, M. Lee, H. Min, S. Kim, J. Yang, H. Kweon, W. Lee, D. H. Kim, J.-H. Choi, D. Y. Ryu, M. S. Kang, B. Kim, J. H. Cho, *Nat. Commun.*, 2020, **11**, 1520.
4. M. S. Jang, S. Yoon, K. M. Sim, J. Cho, D. S. Chung, *J. Phys. Chem. Lett.*, 2018, **9**, 8.
5. D. K. Neethipathi, H. S. Ryu, M. S. Jang, S. Yoon, K. M. Sim, H. Y. Woo, D. S. Chung, *ACS Appl. Mater. Interfaces*, 2019, **11**, 21211.
6. S. Yoon, G. S. Lee, K. M. Sim, M.-J. Kim, Y.-H. Kim, D. S. Chung, *Adv. Funct. Mater.*, 2020, **31**, 2006448.
7. M. Daanoune, R. Clerc, B. Flament, L. Hirsch, *J. Appl. Phys.*, 2020, **127**, 055502.
8. R. Häusermann, E. Knapp, M. Moos, N. A. Reinke, T. Flatz, B. Ruhstaller, *J. Appl. Phys.*, 2009, **106**, 104507.
9. V. D. Mihailetchi, H. Xie, B. de Boer, J. A. Koster, P. W. M. Bom, *Adv. Funct. Mater.*, 2006, **16**, 699.